

# RHEOLOGY, PROCESSING AND ELECTRICAL PROPERTIES OF MULTIWALL CARBON NANOTUBE/POLYPROPYLENE NANOCOMPOSITES

*Semen B. Kharchenko<sup>1</sup>, Kalman B. Migler<sup>1</sup>, Jack F. Douglas<sup>1</sup>, Jan Obrzut<sup>1</sup> and Eric A. Grulke<sup>2</sup>*

<sup>1</sup>*National Institute of Standards and Technology, Gaithersburg, MD 20899-8544,*

<sup>2</sup>*Materials Research Science & Engineering Center, University of Kentucky, Lexington, KY  
40506*

## Abstract

Dispersal of a relatively small concentration (about 1 % volume fraction) of multiwall carbon nanotubes (MWNT) into polypropylene (PP) is found to cause large and complex changes in nanocomposite transport properties. Specifically, both the shear viscosity  $\eta$  ( $\dot{\gamma}$ ) and electrical conductivity  $\sigma$  ( $\dot{\gamma}$ ) of the MWNT nanocomposites decrease strongly with shear rate and, moreover, these dispersions exhibit impressively large and negative normal stresses. Additionally, when extruded, MWNT nanocomposites shrink rather than swell. We associate these flow-induced property changes with the formation of non-equilibrium, percolated nanotube network structures.

## Introduction

Onsager [1] first explained the tendency of highly anisotropic rod-like and plate-like particles (e.g., tobacco mosaic virus and clay particles in solution) to form orientally ordered nematic phases and since this work his insights have been refined into a rich and technologically significant theory of liquid crystalline material properties and phase transitions [2]. The applicability of this theory to ensembles of extended objects becomes questionable, however, when the objects become so large that Brownian motion becomes insignificant and the attainment of the equilibrium thus impossible. This condition arises, for example, when highly extended particles are placed in a highly viscous matrix, precisely the characteristics of carbon nanotube and exfoliated clay polymer nanocomposites. Such materials are inherently out of equilibrium and can be expected to exhibit properties distinct from their equilibrium liquid crystalline counterparts. Moreover, the properties of these materials should depend on flow history, leading to some potential to actuate the material from one state to another under the same nominal thermodynamic conditions.

While the relevance of thermodynamic theory is questionable for this type of nanocomposite, interparticle interactions must remain a prominent feature for these materials. Moreover, this interference must occur at low 'overlap concentrations'. What kind of material state (or

states) should emerge from this collective interparticle interference under such non-equilibrium conditions?

Our observations below suggest that the distribution of MWNT in PP leads to a relatively uniformly dispersed material without the necessity of utilizing surfactants (Figure 1). Moreover, our data seem to suggest that the MWNT form a random network that interpenetrates the PP matrix. This network structure is robust and can also be observed in the course of burning the polymer nanocomposite [3]. After burning the polymer nanocomposite we are left with a nanotube structure of remarkable uniformity.

Our findings demonstrate that these materials are similar to other materials pressed into a non-equilibrium solid ('gel') state through deformation of particles into a disordered state having a concentration greater than random close packing (e.g., foams, emulsions, pastes, multiarm star polymers, etc). While the carbon nanotubes are highly rigid, they can deflect (and, of course, break!) substantially in response to intertube interactions under processing conditions to form a disordered web-like structure of substantial mechanical integrity. What kind of transport properties can be expected from this state of matter, beyond the obvious expectation of an increased stiffness (viscosity) and of increased electrical and thermal conductivity? The present paper explores this basic question.

## Experimental Procedure

The MWNTs were grown in a chemical vapor deposition reactor by the catalytic decomposition of hydrocarbons [4], and MWNT/PP blends were formed with volume fractions ( $\phi$ ) ranging from 0.0025 to 0.15 by melt blending MWNT and PP pellets using a Haake PolyLab mixer [5] operating at 2.1 rad/s and a barrel temperature of 180 °C [3]. To probe the role of MWNTs on viscoelasticity of MWNT/PP blends, dynamic frequency and steady shear experiments were carried out on Advanced Rheometric Expansion System (ARES) [5] with a 25 mm parallel plate geometry in the 180 °C to 220 °C temperature range. The measurement temperature was controlled by gaseous nitrogen at all times.

The shear flow of MWNT/PP nanocomposites can be characterized by strongly dominating hydrodynamic forces

and by the absence of inertia effects, as evidenced from the huge Péclet and vanishing small Reynolds numbers:

$$Re = \frac{VD}{\eta} \approx 10^{-8} - 10^{-11} \quad (1)$$

$$Pe = \frac{\dot{\gamma}D_r}{D_r} \approx 10^{13} - 10^{16} \quad (2)$$

where:  $D_r = \frac{\beta D_{ro}}{(nL^3)^2}$  is the rotary diffusion coefficient and

$D_{ro} = \frac{kT \ln(a_r)}{(3\pi\eta L^3)}$  is the rotary diffusion coefficient of an

isolated rod of high aspect ratio [6]. Here,  $\eta$  is the viscosity of polypropylene,  $\dot{\gamma}$  is the shear rate (or oscillatory frequency),  $V$  is the characteristic fluid velocity,  $D$  is the characteristic geometrical dimension,  $L$  is the nanotube length,  $a_r$  is the nanotube aspect ratio (taken to be approximately 400 [3]),  $\beta$  is set to unity [6], and  $n$  is the number density of nanotubes. Because of the high volume fractions of the nanotubes and their extended nature, lubrication forces prevail in these fluids, similarly to studies on highly concentrated suspensions of spherical aggregates [7-13]. This must be reflected in the bulk rheological response of the nanocomposites, which appears to greatly depend on the complex steric nanotube-nanotube interactions [12, 13].

Carbon nanotubes are known to be highly electrically conductive and their most important applications have been in the modification of material electrical conductivity [14]. There have been several studies of the electrical conductivity of these types of nanocomposites [15-17], but none has considered simultaneous rheology and conductivity measurements. Complex impedance measurements of our MWNT/PP nanocomposites were carried out in the AC frequency range of 40 Hz to 10 MHz using an Agilent 4294A Precision Impedance Analyzer (PIA) [5]. The output AC voltage was  $(0.5 \pm 0.005)$  V (unless otherwise noted, the  $\pm$  represents standard uncertainties of the measured values and refers to one standard deviation of the observed value), and the measurements were performed at 200 °C. The disks were connected to a 4-Terminal-pair-1-m 50  $\Omega$  high-temperature coaxial extension adapter. The relative standard uncertainty of impedance was within the manufacturer's specification for the PIA.

## Results and Discussions

Figure 2 shows the frequency dependence of the storage ( $G'$ ) and viscous ( $G''$ ) modulus for the pure PP and all of the MWNT/PP nanocomposites. It is apparent that both the elasticity of the nanocomposite and its ability to dissipate the viscous energy increases with  $\phi$ . However, the former increases with the greater rate. For the 0.25 % MWNT/PP blend, the frequency dependence of  $G'$  is observed to be almost indistinguishable from that of the PP (except at the lowest frequencies), but  $G'$  of the 0.5 % MWNT/PP blend

shows a pronounced increase. When  $\phi$  reaches 0.01,  $G'$  becomes nearly independent of frequency, and when  $\phi \geq 0.025$  both moduli develop a well-defined plateau. Additionally, when  $\phi \geq 0.005$  the MWNT/PP rheology appears to be thermorheologically complex, and the time-temperature superposition fails for these materials. This is demonstrated for 1 % MWNT/PP nanocomposite tested at 180 °C, 200 °C and 220 °C (Figure 3a). Moreover, when  $\phi \geq 0.005$  the empirical Cox-Merz rule also does not apply (Figure 3b), suggesting that highly interactive nanotubes start interlocking into a network structure [18].

In part, we have witnessed the effect of complex nanotube-nanotube interactions on the shear stress, yet from the fundamental and pragmatic point of view even more interesting would be to observe this effect on the normal stresses. Shear dependence of the normal force (tested using parallel plates) as a function of the packing density of the MWNT in nanocomposites is summarized in Figure 4. While for low  $\phi$  ( $N_1 - N_2$ ) is small and positive, for  $\phi \geq 0.025$  it is large and negative. The magnitude of ( $N_1 - N_2$ ) also seems to scale with  $\phi$ .

Die swell is an obvious processing characteristic influenced by the magnitude and sign of the normal stress. One might expect that when a MWNT/PP nanocomposite, developing a negative normal stress, is extruded through the die, will not exhibit any die swell. We tested this using a 2.5 % MWNT/PP sample for which both ( $N_1 - N_2$ ) and  $N_1$  were found to be negative in the range of shear rates studied. Figure 5 clearly shows that the diameter of the nanocomposite extrudate is much smaller than that of the pure polypropylene, and is also smaller than the diameter of the die (ranging from 0.88 to 1.1 fraction of the die diameter). At the same time, extrusion of pure PP at the same conditions produces an enormous swelling (up to 2.5 times) and apparent shape distortions. The change in extrudate geometry is indeed dramatic.

Next, electrical conductivity measurements were performed *in situ* with the rheology measurements in steady shear aiming to gain some insight into the effect of shear field on the evolution of the nanotube network structure. First, we characterize the conductivity 'overlap concentration'  $\phi^*$  of our MWNT/PP nanocomposites in the molten state using electrical conductivity  $\sigma$  measurements at rest (Figure 6).  $\phi^*$  is defined operationally as the concentration  $\phi$  at which  $\sigma$  sharply increases. As it follows from the plot, the conductivity strongly increases for  $\phi^*$  in the range from 0.0025 to 0.0075, which is comparable to earlier reports [16]. This supports the onset of intense nanotube-nanotube interactions observed in the rheology measurements. We note that the geometrical percolation threshold for overlapping needles in the range of  $\phi$  between 0.01 and 0.001 corresponds to an aspect ratio range between 100 and 1000 [19]. Independent measurement of the aspect ratio of our nanotubes using transmission electron microscopy (TEM) indicates an aspect ratio near

1000 before processing and between 300 and 400 after the processing.

The *in situ* electro-rheology measurements are shown in Figure 7. In this figure the shear rate dependence of the amplitude of the complex conductivity ( $\sigma$ ) for 2.5 % MWNT/PP blend is plotted against the AC frequency. It is apparent that  $\sigma$  is AC frequency independent, but the efficacy of the nanotube network to transmit electric charges decreases with increased  $\dot{\gamma}$  following a characteristic power law decay with an exponent of  $-0.66$ . A similar effect of  $\dot{\gamma}$  is seen in the phase of the AC signal (not shown), which was noted to gradually deviate from zero values. Such a response suggests that the shear field affects the contact distribution of nanotubes in the network, leading to a capacitive-like behavior of the nanocomposite.

## Conclusion

Beyond relatively low concentrations, estimated to be in the range  $0.0025 \geq \phi \geq 0.0075$ , rheological and electrical conductivity properties of MWNT/PP nanocomposites change dramatically as the carbon nanotubes begin to interact strongly. It seems likely that when the percolation threshold of the tubes is exceeded, the transition from the liquid-like to solid-like response of MWNT/PP nanocomposites can be understood by the formation of a non-equilibrium state [20-22]. This is similar to observations in other systems, such as colloidal suspensions [23, 24] and granular media [25, 26] that are also known to exhibit non-equilibrium solid-like rheological properties.

Manifestations of the highly non-equilibrium MWNT network are seen in the rheology via increased elasticity, pronounced failure of the time-temperature superposition, and the failure of the Cox-Merz rule. The most salient feature of the non-equilibrium nanotube network structure appears to be its 'resistance' to shear flow observed through the development of negative hydrodynamic stresses in steady shear and through the suppression of the 'die swell' during the extrusion. While percolated nanotubes can act as effective charge carriers, the shear field can strongly modify the MWNT network and deteriorate the nanotube connectivity.

## References

1. Onsager, L., *Ann. NY. Acad. Sci.*, **57**, 627-638 (1949).
2. de Gennes, P. G.; Prost, J., *The Physics of Liquid Crystals*, Second Edition, Clarendon Press, Oxford 1 (1993).
3. Kashiwagi, T.; Grulke, E.; Hilding, J.; Harris, R.; Awad, W.; Douglas, J., *Macromol. Rapid Comm.* **23**, 761-765 (2002).
4. Andrews, R.; Jacques, D.; Rao, A.M.; Derbyshire, F.; Qian, D.; Fan, X.; Dickey, E.C.; Chen, J., *Chem. Phys. Lett.* **303**, 467-474 (1999).

5. Certain equipment, instruments or materials are identified in this paper in order to adequately specify the experimental details. Such identification does not imply recommendation by the National Institute of Standards and Technology nor does it imply the materials are necessarily the best available for the purpose.
6. Powell, R.L., *J. Stat. Phys.* **62**, 1073-1094 (1991).
7. Zarraga, I.E.; Hill, D.A.; Leighton, D.T., *J. Rheol.* **44**, 185-220 (2000).
8. Aral, B. K.; Kalyon, D. M., *J. Rheol.* **41**, 599-620 (1997).
9. Kolli, V. G.; Pollauf, E. J.; Gadala-Maria, F., *J. Rheol.* **46**, 321-334 (2002).
10. Singh, A.; Nott, P. R., *J. Fluid Mech.* **490**, 293-320 (2003).
11. Zarraga, I.E.; Hill, D.A.; Leighton, D.T., *J. Rheol.* **45**, 1065-1084 (2001).
12. Sierou, A.; Brady, J. F., *J. Rheol.* **46**, 1031-1056 (2002).
13. Foss, D. R.; Brady, J. F., *J. Fluid Mech.* **407**, 167-200 (2000).
14. Ebbesen, T. W.; Lezec, H. J.; Hiura, H.; Bennett, J. W.; Ghaemi, H. F.; Thio, T., *Nature* **382**, 54-56 (1996).
15. Sandler, J. K. W.; Kirk, J. E.; Kinloch, I. A.; Shaffer, M. S. P.; Windle, A. H., *Polymer* **44**, 5893-5899 (2003).
16. Barrau, S.; Demont, P.; Peigney, A.; Laurent, C.; Lacabanne, C., *Macromolecules* **36**, 5187-5194 (2003).
17. Bin, Y. Z.; Kitanaka, M.; Zhu, D.; Matsuo, M., *Macromolecules* **36**, 6213-6219 (2003).
18. Macosko, C. W., *Rheology: principles, measurements, and applications*, New York: VCH (1994).
19. Garboczi, E. J.; Snyder, K. A.; Douglas, J. F.; Thorpe, M. F., *Physical Review E* **52**, 819-828 (1995).
20. Liu, A. J.; Nagel, S. R., *Nature* **396**, 21-22 (1998).
21. Trappe, V.; Prasad, V.; Cipelletti, L.; Segre, P. N.; Weitz, D. A., *Nature* **411**, 772-775 (2001).
22. D'Anna, G.; Gremaud, G., *Nature* **413**, 407-409 (2001).
23. Faraudo, J. *Phys. Rev. Lett.* **89**, (2002).
24. Lootens, D.; Van Damme, H.; Hebraud, P., *Phys. Rev. Lett.* **90**, (2003).
25. To, K.; Lai, P. Y.; Pak, H. K., *Phys. Rev. Lett.* **86**, 71-74 (2001).
26. Longhi, E.; Easwar, N.; Menon, N., *Phys. Rev. Lett.* **89**, (2002).

## Key Words

Nanotube, rheology, normal stress, conductivity.

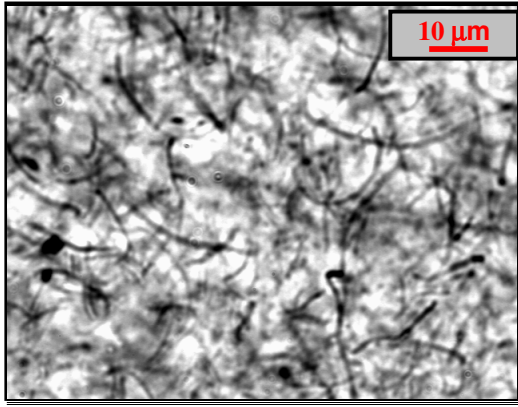


**Figure 1.** This optical microscopy image of 0.25 % MWNT/PP nanocomposite reveals high polydispersity in MWNT length and irregularities in shape.

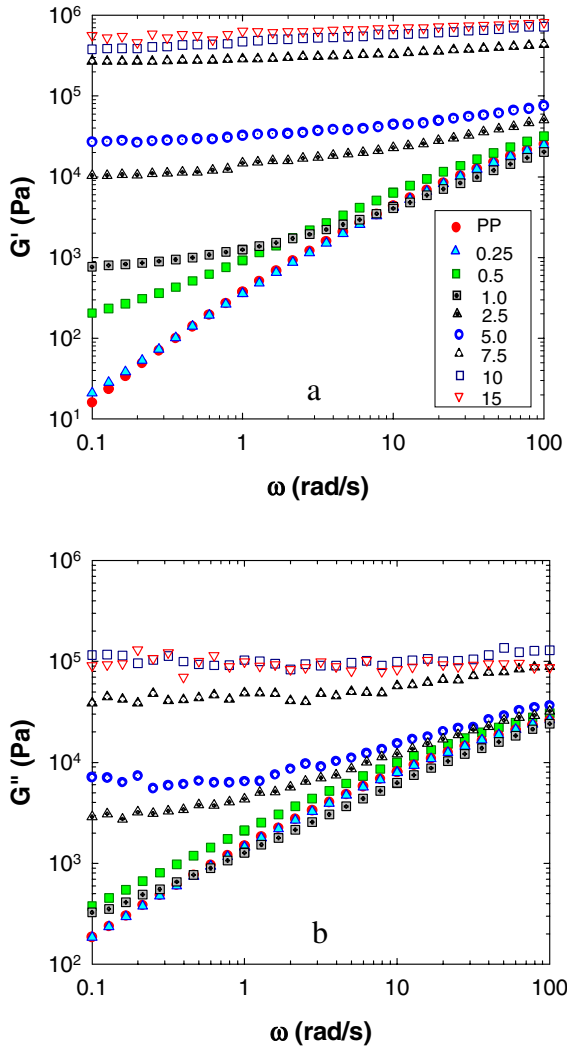
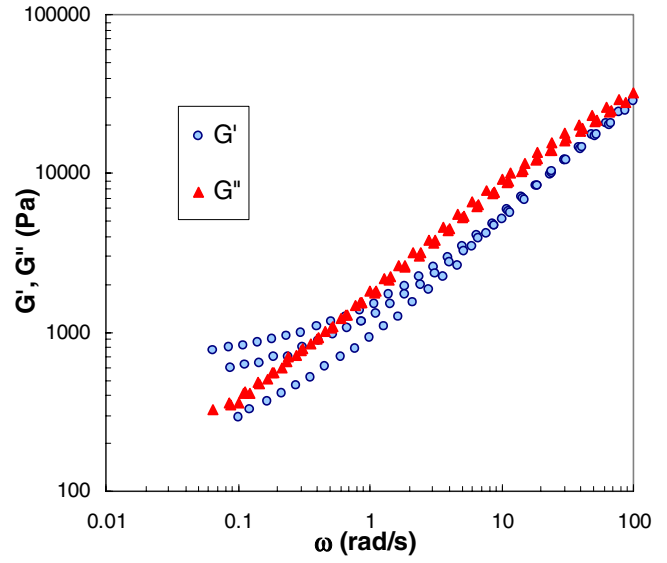
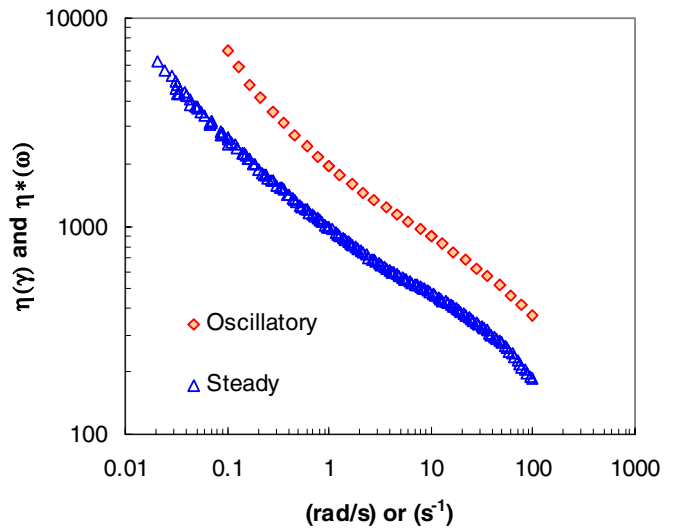


**Figure 2.** Effect of MWNT content on: a)  $G'$  and b)  $G''$ .  $T = 220\text{ }^{\circ}\text{C}$ .



(a)



(b)

**Figure 3.** Manifestation of the interactive nanotube microstructure (demonstrated here for 1% MWNT/PP nanocomposite) through: a) Failure of the time-temperature superposition ( $T_{\text{ref}} = 180\text{ }^{\circ}\text{C}$ ); b) Violation of the Cox-Merz rule (evaluated at  $T = 200\text{ }^{\circ}\text{C}$ ).

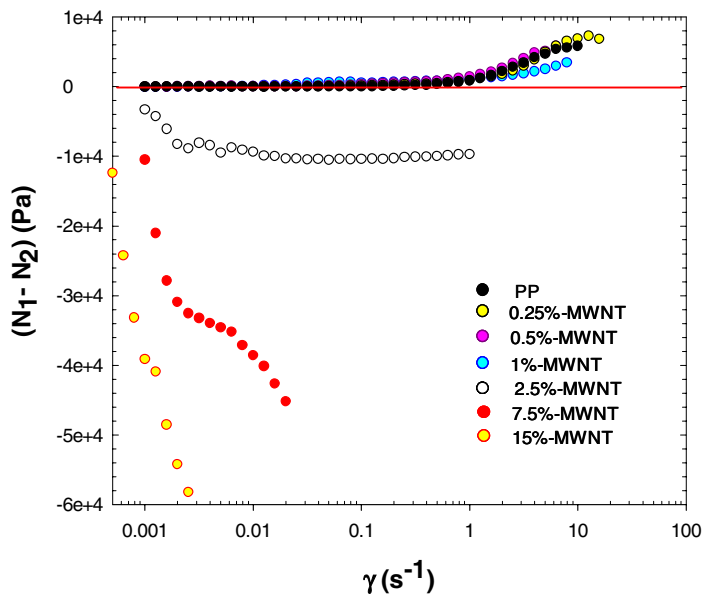


**Figure 4.** Effect of the MWNT content on the normal force.  $T = 220\text{ }^{\circ}\text{C}$ .

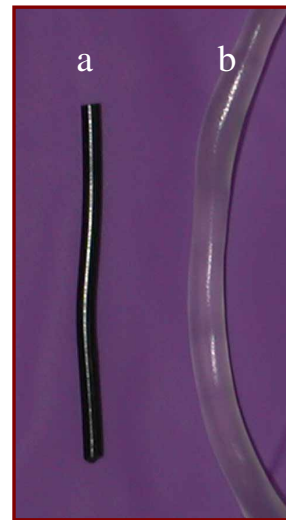


**Figure 5.** Extrusion of: a) 2.5 % MWNT/PP; b) PP.

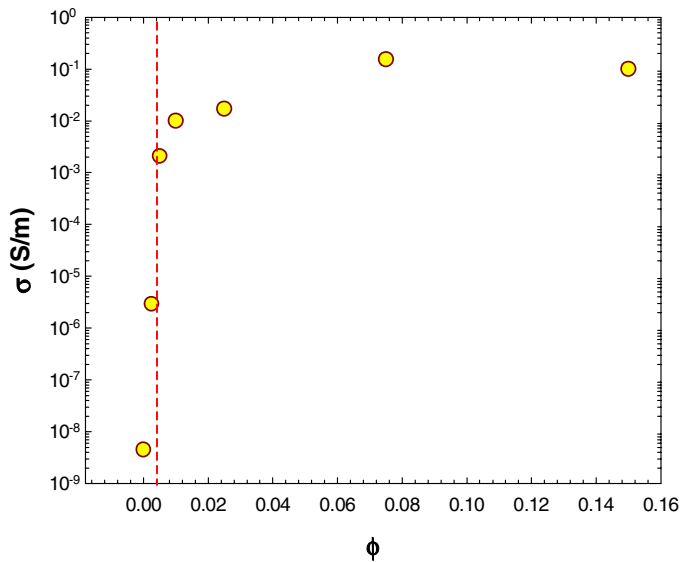


**Figure 6.** Estimation of the electrical percolation threshold.  $T = 200\text{ }^{\circ}\text{C}$ .

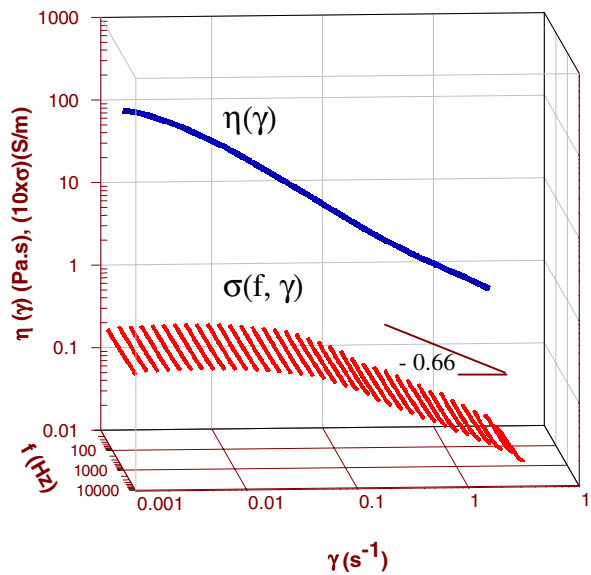


**Figure 7.** Shear rate dependence of the electrical conductivity and viscosity.  $T = 200\text{ }^{\circ}\text{C}$ .